

Tissue distribution of malic enzyme-NADP⁺ in *D. melanogaster* imaginal discs

John D. Finkbohner^{1,*}, Glenn N. Cunningham¹, and David T. Kuhn²

Department of Chemistry¹ and Department of Biological Sciences², University of Central Florida, Orlando, Florida 32816, USA

Summary. The spatial distribution patterns of malic enzyme-NADP⁺ (ME) in *Drosophila melanogaster* imaginal discs and other structures were demonstrated histochemically. Staining in the imaginal discs was limited to specific areas where intense reactions occurred primarily in differentiating structures. The eye-antennal disc possessed the most distinctive staining pattern. The ommatidial preclusters and clusters of the eye portion both stained, with heavier deposition in mature clusters. Staining in the preclusters closest to the morphogenetic furrow (MF) was obscured by a band of stained cells on either side of the MF that extends dorso-ventrally across the disc. The ME low activity mutant *Men^{NC1}* showed a dramatic reduction in staining of this band of cells but had no visible effect on eye morphogenesis. The larval optic nerve which traverses the entire length of the eye-antennal disc was a consistently stained feature. Two structures specifically stained in the leg discs. The most prominent was the chordotonal organ, while the second was a larval nerve extending the length of the disc. Limited staining was observed in the wing disc. No ME staining could be detected in the labial disc or haltere disc. Even though the genital discs did not stain for ME, the enzyme was induced sometime during the pupal stage since intense staining was noted in several adult internal genital disc derived structures. In general, ME staining in imaginal discs was associated with structures from the nervous system.

Key words: Malic enzyme – Distribution patterns – Imaginal discs – *Drosophila melanogaster*

Introduction

Each imaginal disc of *Drosophila* differentiates specific adult structures during pupariation as shown by transplantation studies (Nöthiger 1972). The biochemical commitment of certain imaginal cell groups to specific developmental pathways can be traced throughout larval development into early pupal development by following enzyme activity

distribution profiles (Gehring 1976; Kuhn and Cunningham 1977a; Sprey et al. 1982). The visualization of these patterns allows us to relate enzyme staining to imaginal disc fate maps (Bryant 1978).

Imaginal discs have been used as a model system for developmental studies for several years. The discs are divided into compartments, which are specific regions inferred by clonal restrictions in the pattern of cuticular structures (Garcia-Bellido et al. 1976). The developmental fate of each area within an imaginal disc has been determined by transplanting disc fragments and analyzing the differentiated cuticular structures (Bryant 1978). Distribution of some enzymes within the imaginal discs appears to: 1) respect some clonally restrictive borders (Kuhn et al. 1983); 2) mark specific presumptive structures within an area of a disc (Cunningham and Kuhn 1981); and 3) identify regions specifically transformed by various homeotic mutations (Kuhn and Cunningham 1976, 1977a; 1977b).

The use of enzyme markers in the study of developmental commitment in *Drosophila melanogaster* imaginal discs has undergone rapid expansion over the past several years (reviewed by Silvert and Fristrom 1980). The first enzyme in *Drosophila melanogaster* for which a histochemical stain was applied to the imaginal discs was the cell intrinsically expressed aldehyde oxidase (AO) (Janning 1972; 1973). Since that time, AO has been used to augment data derived from transplantation studies. The histochemical information can give us a more complete picture of imaginal disc differentiation. Other enzyme markers previously studied in *Drosophila melanogaster* include: isocitrate dehydrogenase-NADP⁺ dependent (Cunningham and Kuhn 1981); glucose-6-phosphate dehydrogenase (Cunningham et al. 1983); and succinate dehydrogenase (Lawrence 1981).

A histochemical stain for malic enzyme-NADP⁺ dependent (ME-NADP; EC 1.1.1.40) has been developed and utilized in the study of cellular differentiation in *Drosophila melanogaster*. ME-NADP is a cytoplasmic enzyme of *Drosophila melanogaster* which is coded for by the *Men⁺* gene located in the right arm of chromosome 3 at 51.7 (Voelker et al. 1981; Doane and Treat-Clemons 1982). ME-NADP is a decarboxylating oxidoreductase which is important in the generation of NADPH for lipid biosynthesis (Geer et al. 1976; Geer et al. 1979b). Patterns of ME-NADP staining should prove useful for the study of cell and tissue commitments on an enzymatic level, since it can be shown that the staining patterns are specific and remarkably repeatable.

Offprint requests to: D.T. Kuhn, Department of Biological Sciences, University of Central Florida, Orlando, Florida 32816, USA

* *Present address:* J.D. Finkbohner, Biochemistry Program, Pennsylvania State University, 108 Althouse Laboratory, University Park, Pennsylvania 16802, USA

Materials and methods

An Oregon-R-C wild type strain, tumorous-head stocks (*tuh-1*; *tuh-3*) and a low ME mutant strain (*Men^{NC1}*) of *Drosophila melanogaster* were used in our study of ME-NADP distribution patterns. Descriptions of mutants and stocks are given in Lindsley and Grell (1968) and Williamson (1982). For brevity ME-NADP will be presented henceforth as ME. All stocks were maintained at 25° C on a medium consisting of agar-cornmeal-yeast-dextrose-sucrose with phosphoric acid and propionic acid added as mold inhibitors.

Imaginal discs from late third instar larvae were removed in a modified *Drosophila* Ringer's solution (Cunningham et al. 1983) buffered at pH 6.9 with 0.02 M 3-(N-morpholino)propanesulfonic acid (MOPS) and incubated with a fixation solution containing 1% glutaraldehyde in a pH 4.2 acetate buffered modified *Drosophila* Ringer's solution at 4–8° C. The glutaraldehyde treatment was limited to thirty seconds to minimize enzyme inactivation. The level of fixation can be increased by prolonging the fixation time. However, this results in a greater loss of ME activity, with no change in the staining pattern. After fixation the tissue was immediately transferred to a 0.3 M tris-(hydroxymethyl)aminomethane-HCl (Tris) buffer rinse solution at pH 6.9 between 4–8° C. The tissue remained in the Tris rinse solution for 5–15 minutes, which removed the remaining unreacted glutaraldehyde. This eliminates staining for aldehyde oxidase (AO), and is best accomplished by dissecting the tissue away from the larval hypoderm, thereby allowing the Tris solution greater contact with the fixed tissue.

The tissue was then incubated in a humid chamber at 35° C in a staining solution which contained final concentrations of 4.8 mM MnCl₂; 0.2 M Tris-HCl, pH 8.05; 0.2 mg/ml phenazine methosulfate; 2.6 mg/ml nitrobluete-trazolium; 3.7 mM β-nicotinamide adenine dinucleotide phosphate oxidized form (NADP⁺); 8 mg/ml polyvinyl alcohol; and 25.4 mM L-malate disodium salt. The staining times varied from 10–30 min depending on the tissue being stained and the age of the larva from which the tissue was obtained. The staining procedure was completed in the dark to avoid light-induced precipitation of formazan.

The reaction was terminated with a rinse in a solution of 3:1 ethanol:acetic acid for 2–10 min. Tissue was then transferred into a lactophenol solution for further manipulation and storage. The imaginal discs or other tissues were placed on microscope slides in Faure's mounting medium and coverslipped. Representative patterns for each imaginal disc were established by examination of at least 50 of each disc type. Variation between individual discs was minor.

The specificity of the ME staining technique has been demonstrated by the use of the appropriate controls. No staining occurs in imaginal discs when substrate and/or the coenzyme controls are applied to *Drosophila* tissues for a prolonged period of time. The patterns seen are dependent upon the presence of the enzyme, the substrate L-malate and NADP⁺. Phenazine ethosulfate (PES) has been used in a technique to stain electrophoretic gels for ME activity (Geer et al. 1979a). PES was substituted for phenazine methosulfate (PMS) to test the effect on histochemical staining. The PES substitution gave the staining solution seemingly enhanced sensitivity. However, it also resulted in a general light blue non-specific background staining.

The patterns seen using PES are the same as those for the PMS formula. The use of PMS is preferred because of a decrease in the non-specific staining. The use of PES is only necessary in the wing disc due to the low activity in that disc.

Results

Differential distribution of ME can be found in various larval tissues. The intensity of stain deposition in tissue depends on the age of the larva, type of tissue being studied and the length of time the tissue was incubated in the staining solution. There is a general tendency for the highest ME activity levels to be detected in larval adipose and muscle tissue. Because of the visual nature of the results, they will be discussed figure by figure.

Salivary gland. The anterior fat bodies, closely associated with the variably stained salivary gland cells, show high ME activity. The ring of imaginal cells located at the base of each salivary gland shows intense ME staining (Fig. 1A).

Labial disc. After prolonged incubation (30 min) in the staining solution, the labial disc does not demonstrate any observable ME staining (Fig. 1B).

Dorsal prothoracic disc. No ME staining can be found in the imaginal cells that partially encircle the dorsal tracheal trunk, whereas the girdle of larval cells demonstrates intense activity (Fig. 1C). The disc is a ball of cells formed by an outer layer of imaginal cells and a inner layer of larval cells, with the cuticle forming surface of the imaginal cells next to the larval cells (Lamprecht and Remensberger 1966; Madhavan and Schneiderman 1977).

Leg discs. All leg discs are essentially unstained for ME (Fig. 1D, 1E). A notable exception is the heavily stained chordotonal organ which is located near the joint of the prospective femur and tibia (van Ruiten and Sprey 1974). This organ is composed of multiple scolopidia which, as discussed by van Ruiten and Sprey (1974), have sensory neurons as part of their structure. The nerve fiber connecting the first and second leg discs to the ventral ganglion shows intense staining as does the fiber/tracheal branch passing through the region where the first leg discs fuse (Fig. 1D). The leg discs, especially the second and third leg discs, have a darkly staining nerve which has branched fibers spreading over the presumptive tarsal segments 2–5 and claw (see arrow in Fig. 1E).

Abdominal histoblasts. The smaller cells comprising nests of abdominal histoblasts show more staining than the surrounding larval hypoderm cells that are ME positive (Fig. 1F). Nuclei of the imaginal cells are surrounded by ME stained cytoplasm. The nest of abdominal histoblasts is situated next to larval muscles that stain darkly for ME.

Wing disc. The wing disc shows a pattern only upon prolonged staining or after sensitivity enhancement via the substitution of phenazine ethosulfate for phenazine methosulfate in the staining solution. A wing disc from a tumorous-head larva is presented in Fig. 1G. The *tumorous-head* mutation has no known effect on the adult wing. This is the only *Drosophila melanogaster* strain thus far examined that shows such extensive staining in the wing pouch. ME stain-

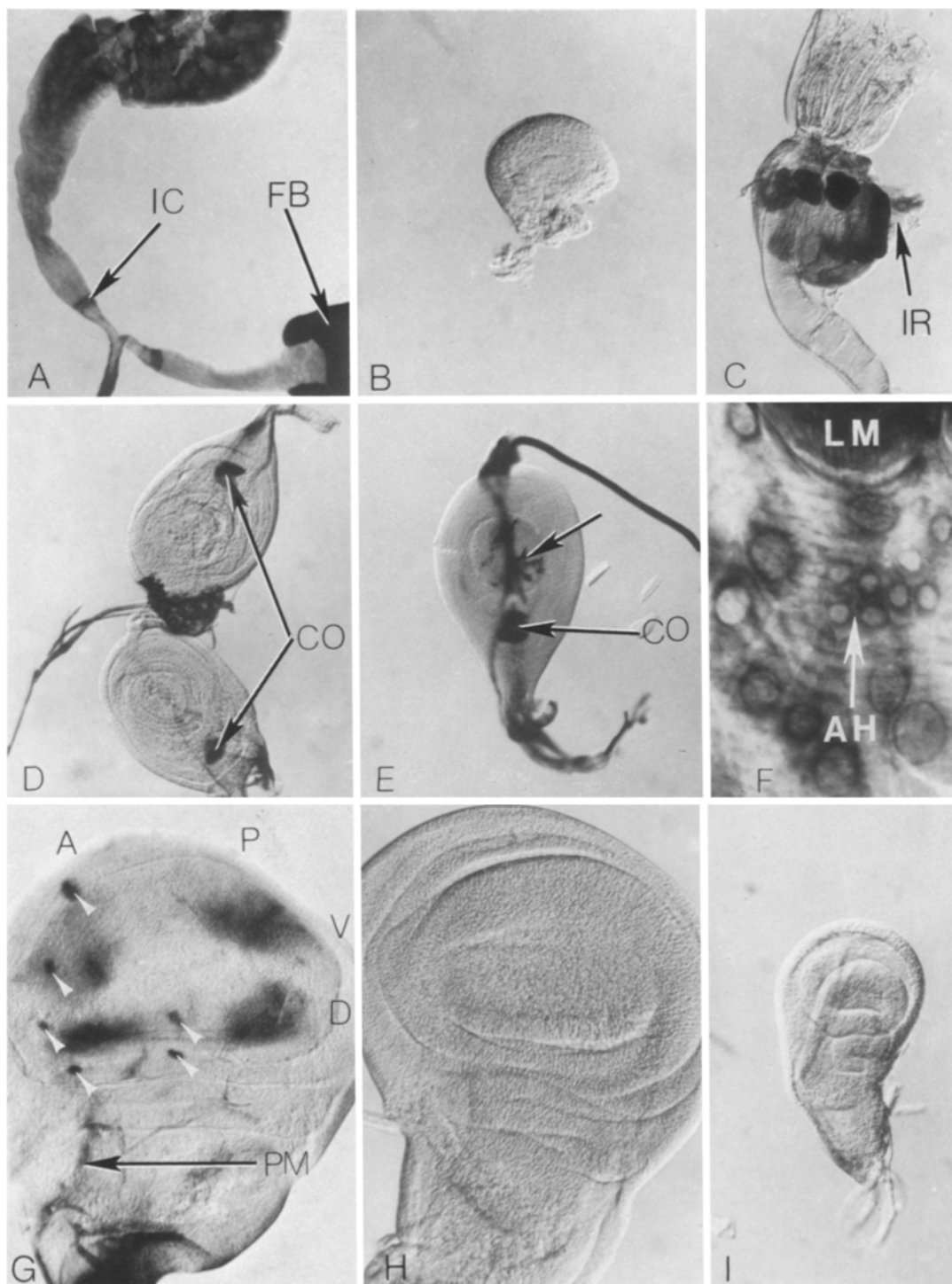


Fig. 1A-I. Malic enzyme (*ME*) staining patterns found in Oregon-R-C imaginal structures. **A** Larval salivary glands $\times 125$. **B** Labial disc $\times 180$. **C** Imaginal ring of cells around the dorsal tracheal trunk $\times 140$. **D**, **E** Prothoracic and mesothoracic leg discs $\times 100$. **F** Nests of abdominal histoblasts $\times 550$. **G** Wing disc from a *tumorous-head* larva $\times 130$. **H** Wild-type wing disc $\times 140$. **I** Haltere disc $\times 130$. *IC*, imaginal ring of salivary glands; *FB*, fat body of salivaries; *IR*, imaginal ring of cells of dorsal prothoracic disc, *CO*, chordotonal organ; *LM*, larval muscles; *AH*, nest of abdominal histoblasts; *PM*, peripodial membrane

ing occurs in the presumptive dorsal and ventral wing blade surfaces both on the anterior and posterior sides. Six specific dots of intense activity occur in/on the disc epithelium on the anterior side of the disc (see arrow heads in Fig. 1G) and some stain is seen in the peripodial membrane. *ME* additionally will stain in the cells of the new tracheal

branch. An Oregon-R-C wing disc, stained for approximately 15 min, is presented in Fig. 1H. No *ME* staining can be seen. Upon prolonged incubation, 30 min, some of the spots of *ME* stain may appear as seen in Fig. 1G as may limited staining in the wing pouch. The stain distribution is identical to that of Fig. 1G.

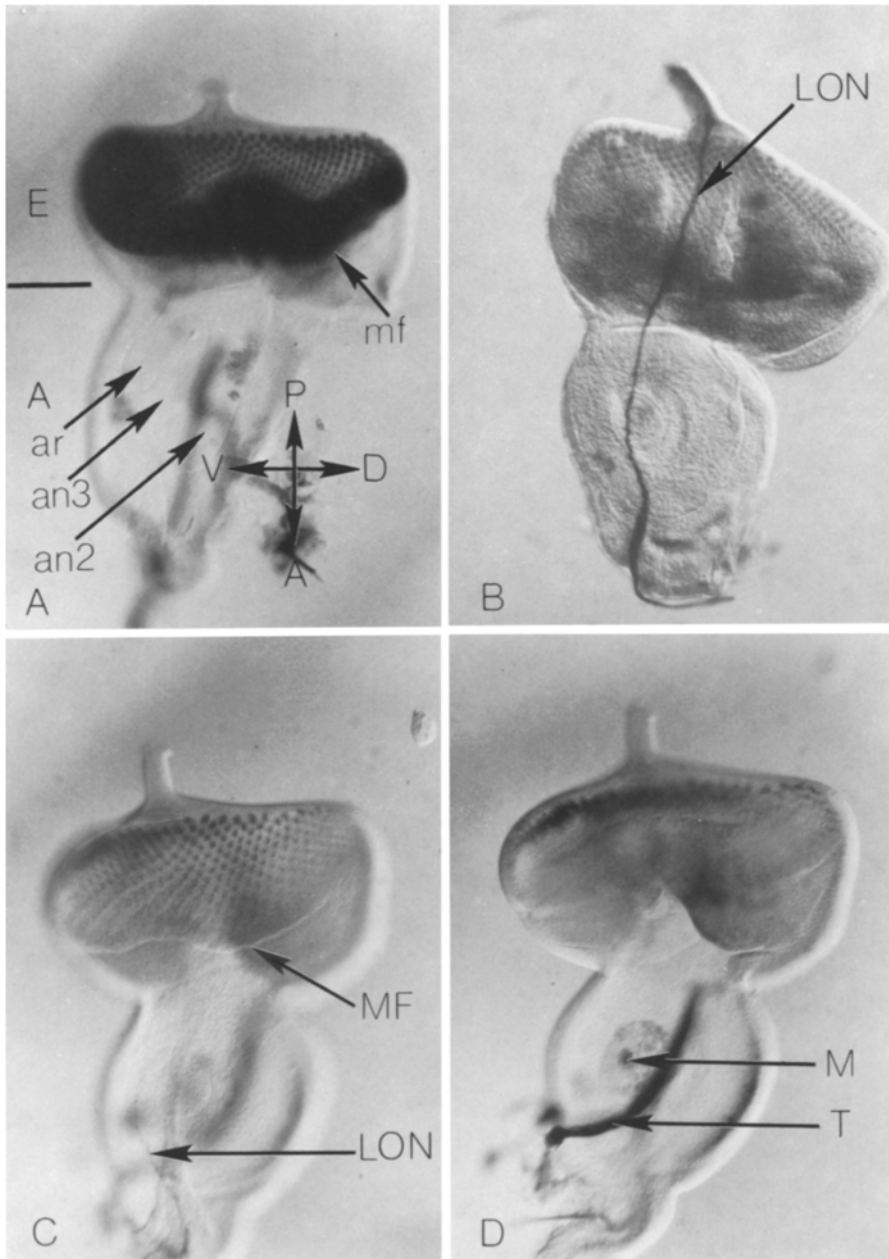


Fig. 2A–D. Pattern of malic enzyme (ME) staining observed in eye-antennal disc. **A** Late third instar $\times 125$. **B** Larval optic nerve in eye disc $\times 145$. **C** and **D** Apical and basal side of *Men^{NC1}* eye-antennal disc $\times 130$. **E**, eye portion of disc; **A**, antennal portion of disc; **P**, posterior; **A** (above arrows) anterior; **V**, ventral; **D**, dorsal; **ar**, rudiment of arista; **an 3**, prospective antennal segment 3; **an 2**, antennal segment 2; **LON**, larval optic nerve; **M**, macrophage-like cells; **MF**, morphogenetic furrow; **T**, trachea

Haltere disc. The haltere disc shows no ME staining upon prolonged staining treatment (Fig. 1I).

Eye-antennal disc. The ommatidial cell clusters in the posterior half of the eye anlage are demarcated by stain while the surrounding hair-nerve group cells and pigment cells lack stain (Fig. 2A). A region of moderate to high activity exists in the anterior half of the eye disc epithelium on either side of the advancing morphogenetic furrow (Fig. 2A, 2B). The presumptive shingle cuticle of the eye disc, which is located near the junction of the eye and antennal portions of the complex does not stain (Bryant 1978). The larval optic nerve, or Bolwig's nerve (Bolwig 1946), stains for ME (Fig. 2B). This nerve is located on the apical side of the disc beneath the peripodial membrane, extending the entire length of the disc complex (Sprey and DePriester 1972).

The antennal disc shows limited ME staining in the disc

epithelium and none in the peripodial membrane (Fig. 2A). Presence of antennal disc cells with high ME activity is variable depending upon developmental stage. Some epithelial cells aligned on the apical side of the second antennal segment stain (Fig. 2A). They can be found in two specific locations closest to the posterior-medial edge of the antennal disc and the anterior-lateral edge of antennal segment 2. Figures 2C and 2D picture the apical side (Fig. 2C) and the basal side (Fig. 2D) of an eye-antennal disc of a low activity mutant for ME (*Men^{NC1}*). The band of ME stained cells extending dorso-ventrally in the area of the morphogenetic furrow (Fig. 2A) is conspicuously absent in the *Men^{NC1}* stained disc. This regulatory mutant reduced ME staining along the furrow substantially. The ommatidial preclusters and clusters stain for ME (Fig. 2C). Staining in the ommatidial preclusters extends to the edge of this sheet of cells as the furrow moves anteriorly through the eye disc. Macrophage-like cells (Ready et al. 1976) occa-

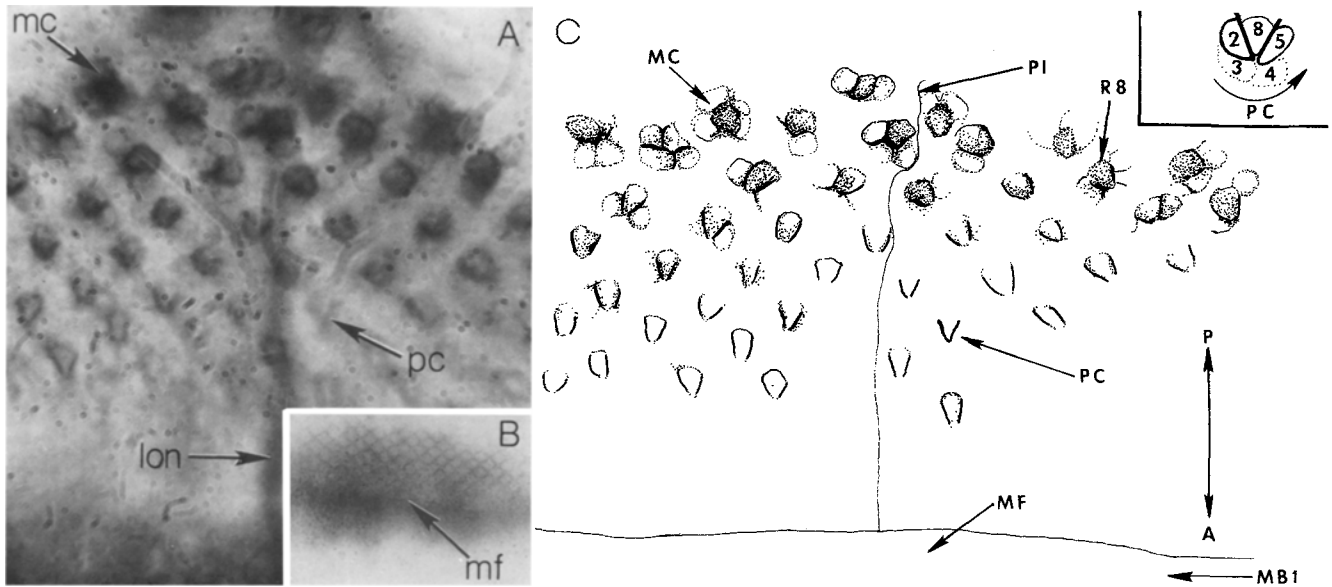


Fig. 3A–C. Malic enzyme (*ME*) stain deposition in differentiating photoreceptor cells from an eye disc in a latter 3rd instar larva. **A** Apical surface of eye disc $\times 400$. **B** Insert in the lower right of **A** is a glucose-6-phosphate dehydrogenase (*G6PD*) stained eye disc prepared following the procedure of Cunningham et al. (1983) $\times 100$. **C** *ME* stain deposition of **A** was traced yielding **C**. *LON*, larval optic nerve; *MF*, morphogenetic furrow; *MC*, mature cluster; *PI*, line of pattern inversion; *PC*, precluster; *MB1*, mitotic band 1; *P*, posterior; *A*, anterior, *R8*, rhabdomere 8; 2, 3, 4, 5, 8, rhabdomeres within a precluster

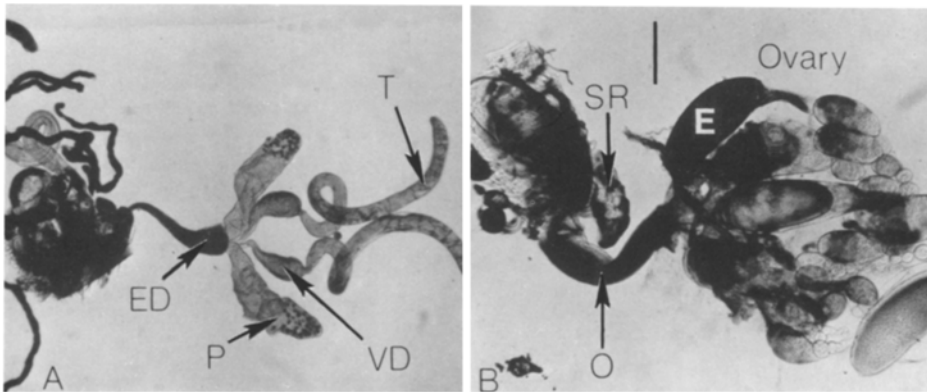


Fig. 4A, B. Malic enzyme (*ME*) staining patterns found in adult genital structures. **A** Adult male genitalia $\times 20$. **B** Adult female genital structures $\times 20$. *ED*, ejaculatory duct; *P*, paragonia; *VD*, vas deferens; *T*, testis; *O*, common oviduct; *SR*, seminal receptacle; *E*, egg

sionally stain for *ME* (Fig. 2D). These cells are located on the basal surface of the presumptive arista-third antennal segment. The remaining stained structure seen in Fig. 2D is the tracheal system attached to the basal side of the disc.

A *ME* stained wild-type eye disc is pictured in Fig. 3A, while an interpretation of that disc is provided in Fig. 3C. Uniform *ME* staining is characteristic of the ultrastructurally similar cells along the morphogenetic furrow (*MF*; Fig. 3C and 3A). Posterior to the *MF*, the differentiating groups of cells comprising ommatidial preclusters stain in a consistent pattern. *ME* stain initially appears on either side of rhabdomere 8 (*R8*), which is flanked by rhabdomeres 2 and 5 (see insert in upper right of Fig. 3C). Preclusters immediately posterior to the *MF* show a characteristic V shaped stain deposition. The base of the V points anteriorly toward the *MF*. As one examines the preclusters in an anterior to posterior direction, a gradual rotation of

cell clusters laterally can be seen on either side of the equatorial line (Fig. 3C). The association of the five rhabdomeres of a precluster, the rotation for the right side of the disc (see arrow) and position of *ME* stain are interpreted in the insert (Fig. 3C). The mirror image of this pattern occurs about the equatorial line [Ready et al. (1976), Fig. 8; Campos-Ortega and Gateff (1976), Fig. 1]. The assumption made here is that rhabdomeres 2, 5, and 8 are those visible in stained whole mounts. Stain for *ME* appears to spread through *R8* prior to being detected in the adjacent rhabdomeres, as observed in the mature ommatidial clusters located on the posterior side of the eye disc (Fig. 3C). Rhabdomeres 1, 6, and 7 are added to the precluster at this time to form each mature cluster (Ready et al. 1976). Figure 3B pictures an eye disc which was stained for glucose-6-phosphate dehydrogenase by the technique of Cunningham et al. (1983). *G6PD* stains on both sides of the *MF*. Rhabdomeres in the preclusters do not specifically stain. Rather,

the stain is found at borders between preclusters/clusters and allows visualization of their square array. An approximate position for the line of pattern inversion for the eye disc in Fig. 3A is drawn in Fig. 3C. The ME stained V rotates on either side of the line. The path of the ME stained larval optic nerve (Fig. 3A) is similar in its position. The larval optic nerve is located in the peripodial membrane, between the epithelial cells of the peripodial membrane and basement lamina.

Adult male genitalia. The testes show differential distribution of ME in the outer layer of large flat cells (Fig. 4A). Similar streaks of stain are found in the oval 3rd instar testes. In some regions, the pattern clearly outlines the cells while other areas of the testes may show variable nonspecific activity. The vas deferens shows low general staining. The paragonia show high activity in the clusters of binucleate cells occurring in the distal regions while the surrounding cells remain unstained. The ejaculatory duct shows variable intense staining with a trend of increasing activity towards the paragonial juncture. The sperm pump remains low in activity while the associated musculature shows high ME activity. In contrast to the extensive ME staining in the adult internal male genitalia was the lack of ME staining in the genital disc, male as well as the female.

Adult female genitalia. The ovaries show highly variable staining in the developing eggs (Fig. 4B). The lateral oviducts show intense ME staining while the common oviduct, seminal receptacle, parovaria and uterus all demonstrate moderate activity. No ME staining occurs in the small 3rd instar larval ovaries.

Discussion

The ME staining technique was applied to a ME low mutant *Men^{NC1}* (Williamson 1982) with the expectation that the imaginal discs and other tissues would not stain for the enzyme. *Men^{NC1}* homozygotes possess approximately 8% of normal whole-organism activity during the late 3rd instar stage (Williamson 1982). Yet, the level of activity in the imaginal discs was sufficient for a moderate staining reaction. The general reduction in stain intensity for *Men^{NC1}* discs did not reflect that anticipated of a 12-fold decrease in whole-organism activity. These data can be interpreted in at least three ways that may not be mutually exclusive. First, the staining technique is extremely sensitive and is capable of detecting very low levels of ME. Secondly, since very little of the ME activity is normally found in the imaginal discs, a general reduction in enzyme activity differentially affecting larval tissue could account for the paradoxical results. Thirdly, modifying genes have accumulated in the strain that have resulted in increased ME levels. The *Men^{NC1}* regulatory mutant (Williamson 1982) selectively reduced levels of ME along the morphogenetic furrow in the eye disc while other parts of the ME staining pattern remained. Therefore, *Men^{NC1}* both reduced ME activity generally for all discs and reduced to the lower limits of detection levels surrounding the morphogenetic furrow. No structural defects were found in the eyes of *Men^{NC1}* adults. Apparently the reduced level/lack of ME activity along the morphogenetic furrow was not crucial for normal differentiation of the ommatidia.

The physiological importance of ME lies in the genera-

tion of the reduced NADPH pool necessary for lipogenesis (Geer et al. 1979b). The distribution of ME was highest in larval muscle, nerve tissue, and adipose tissues, which corresponds to the higher lipid biosynthesis rates within these tissues. The need for ME in nerve tissue is presumably correlated to sphingolipid production demands. Fat cells store various proteins and carbohydrates for utilization in a variety of tissues during development. Therefore, ME in fat cells may be sequestered for storage and later use in other tissues.

The specific staining of the ommatidial preclusters/clusters is not confined to ME. Peanut agglutinin likewise demarcates the same cell groups (Fristrom and Fristrom 1982). The primary and secondary pigment cells surrounding the rhabdomeres did not interact with peanut agglutinin, nor did they stain for ME. It is not clear why both staining techniques are so specific for the differentiating ommatidia. However, these cell groups are among the first of the imaginal cells to show visible differentiation. The precise staining may be associated with cell groups after they have begun to specialize.

Monoclonal antibodies have now been used to further study pattern development in the differentiating eye disc (Zipursky et al. 1984). Features highlighted by the monoclonals are those seen with ME, G6PD and peanut agglutinin. Zipursky et al. (1984) show one monoclonal (MAB22C10) specifically staining the photoreceptor cells as they form posterior to the morphogenetic furrow. Like ME, MAB22C10 stains the larval optic nerve or Bolwig's nerve (Bolwig 1946). A second monoclonal antibody (MAB3E1) precisely stains a band of cells along the morphogenetic furrow with more staining anterior to the furrow. The similarity in staining pattern of MAB3E1 and the zone of reduced ME staining in *Men^{NC1}* discs may be coincidental. However, the general pattern element highlighted with both stains was quite similar, if not the same. A third monoclonal antibody (MAB6D6) stains the walls surrounding each group of rhabdomeres in much the same way that G6PD (Fig. 3C) highlighted the square array. Although staining for different cytoplasmic enzymes provides a more general picture of pattern formation than shown by the specific monoclonal antibodies, the developmental patterns revealed are the same.

The ME patterns are different from those reported for other enzyme markers. For example, in the pouch of the mature wing disc, the enzyme markers, aldehyde oxidase (AO, Kuhn and Cunningham 1978), NADP⁺ dependent-isocitrate dehydrogenase (ICDH, Cunningham and Kuhn 1981), and glucose-6-phosphate dehydrogenase (G6PD, Cunningham et al. 1983) delineate compartment borders in some way. ME is the only enzyme we have studied in *D. melanogaster* that does not stain these features of the wing disc.

Staining of the developing photoreceptor cells and chorodonal organs of leg discs by ME remains unique among the enzymes for which histochemical techniques have been applied. It is striking that ME stains very early precursors of neural-sensory-type cells.

Acknowledgements. The authors thank Dr. Anne Fausto-Sterling and Dr. Dianne Fristrom and Dr. Th. E. Sprey for their thoughtful comments on the manuscript. Dr. Michael Bentley is thanked for sending us the *Men^{NC1}* mutant. This work was supported by NIH Grant R01 AG-01846 and NSF Grant PCM-8302104.

References

- Bolwig N (1946) Senses and sense organs of the anterior end of the house fly larva. *Vidensk Medd fra Dansk Naturh Foren Bd* 109:80–212
- Bryant PJ (1978) Pattern formation in imaginal discs. In: Ashburner M, Wright TRF (eds) *The genetics and biology of Drosophila*. Academic Press, New York and London, pp 229–335
- Campos-Ortega JA, Gateff EA (1976) The development of ommatidial patterning in metamorphosed eye imaginal disc implants of *Drosophila melanogaster*. *Wilhelm Roux's Arch* 179:373–392
- Cunningham GN, Kuhn DT (1981) Tissue distribution of isocitrate dehydrogenase in *Drosophila melanogaster*. *Insect Biochem* 11:277–285
- Cunningham GN, Smith NM, Makowski MK, Kuhn DT (1983) Enzyme patterns in *D. melanogaster* imaginal discs: Distribution of glucose-6-phosphate and 6-phosphogluconate dehydrogenase. *Mol Gen Genet* 191:238–243
- Doane WW, Treat-Clemons LG (1982) Biochemical loci of the "fruit fly" (*Drosophila melanogaster*). *Drosoph Inf Serv* 58:41–59
- Fristrom DK, Fristrom JW (1982) Cell surface binding sites for peanut agglutinin in the differentiating eye disc of *Drosophila*. *Dev Bio* 92:418–427
- Garcia-Bellido A, Ripoll P, Morata G (1976) Developmental compartmentalization in the dorsal mesothoracic disc of *Drosophila*. *Dev Bio* 48:132–147
- Geer BW, Kamiak SM, Kidd KR, Nishimura RA, Yemm SJ (1976) Regulation of the oxidative NADP enzyme tissue levels in *Drosophila melanogaster*. I. Modulation by dietary carbohydrate and lipid. *J Exp Zool* 195:15–32
- Geer BW, Krochko D, Williamson JH (1979a) Ontogeny, cell distribution and the physiological role of NADP-malic enzyme in *Drosophila melanogaster*. *Biochem Gen* 17:867–879
- Geer BW, Krochko D, Oliver MJ, Walker VK, Williamson JH (1979b) A comparative study of NADP-malic enzymes from *Drosophila* and chick liver. *Comp Biochem Physiol* 65B:25–34
- Gehring WJ (1976) Determination of primordial disc cells and the hypothesis of stepwise determination. In: Lawrence PA (ed) *Insect development. The 8th Symposium of the Royal Entomological Society of London*. Blackwell Scientific Publications, London, pp 99–108
- Janning W (1972) Aldehyde oxidase as a cell marker for internal organs in *Drosophila melanogaster*. *Die Naturwissenschaften* 59:516–517
- Janning W (1973) Distribution of aldehyde oxidase activity in imaginal discs of *Drosophila melanogaster*. *Drosoph Inf Serv* 50, 151–152
- Kuhn DT, Cunningham GN (1976) Aldehyde oxidase activity in the tumorous head strain of *Drosophila melanogaster*. *Dev Biol* 52:43–51
- Kuhn DT, Cunningham GN (1977a) Aldehyde oxidase compartmentalization in *Drosophila melanogaster* wing imaginal discs. *Science* 196:875–877
- Kuhn DT, Cunningham GN (1977b) Aldehyde oxidase distribution in haltere discs of homoecotic bithorax mutants in *Drosophila melanogaster*. *Mol Gen Genet* 150:37–42
- Kuhn DT, Cunningham GN (1978) Aldehyde oxidase distribution in *Drosophila* imaginal discs, histoblasts and rings of imaginal cells. *J Exp Zool* 204:1–10
- Kuhn DT, Fogerty SC, Eskens AAC, Sprey ThE (1983) Developmental compartments in the *Drosophila melanogaster* wing disc. *Dev Biol* 95:399–413
- Lamprecht J, Remensberger P (1966) Polytöne chromosomen im bereiche der prothoracal-dorsal-imaginalscheibe von *Drosophila melanogaster*. *Experientia* 22:293–294
- Lawrence PA (1981) A general cell marker for clonal analysis of *Drosophila* development. *J Embryol Exp Morphol* 64:321–332
- Lindsley DL, Grell EH (1968) *Genetic variations of Drosophila melanogaster*. Carnegie Inst Wash Pub 627
- Madhavan M, Schneiderman H (1977) Histological analysis of the dynamics of growth of imaginal discs and histoblast nests during the larval development of *Drosophila melanogaster*. *Wilhelm Roux's Arch* 183:269–305
- Nöthiger R (1972) The larval development of imaginal discs. In: Ursprung H, Nöthiger R (eds) *The biology of imaginal discs*. Springer, Berlin Heidelberg New York, pp 1–34
- Ready DF, Hanson TE, Benzer S (1976) Development of the *Drosophila* retina, a neurocrystalline lattice. *Dev Biol* 53:217–240
- Sprey ThE, DePriester W (1972) Myofilaments in the lemnoblast cells of the larval optic nerve in *Calliphora erythrocephala*. *Neth J Zool* 22:351–354
- Sprey ThE, Eskens AAC, Kuhn DT (1982) Enzyme distribution patterns in the imaginal wing disc of *Drosophila melanogaster* and other diptera: A subdivision of compartments into territories. *Wilhelm Roux's Arch* 191:301–308
- Silvert DJ, Fristrom JW (1980) Biochemistry of imaginal discs: retrospect and prospect. *Insect Biochem* 10:341–355
- van Ruiten ThM, Sprey ThE (1974) The ultrastructure of the developing leg disk of *Calliphora erythrocephala*. *Z Zellforsch* 147:373–400
- Voelker RA, Ohnishi S, Langley CH, Gausz J, Gyurkovics H (1981) Genetic and cytogenetic studies of malic enzyme in *Drosophila melanogaster*. *Biochem Genet* 19:525–534
- Williamson JH (1982) *Men^{NC1}*: A putative regulatory mutant of NADP-malic enzyme in *Drosophila melanogaster*. *Can J Genet Cytol* 24:409–416
- Zipursky SL, Venkatesh TR, Teplow DB, Benzer S (1984) Neuronal development in the *Drosophila* retina: Monoclonal antibodies as molecular probes. *Cell* 36:15–26

Received May 9, 1984

Accepted in revised form November 12, 1984